The Design, Fabrication, and Testing of Corrugated Silicon Nitride Diaphragms

Patrick R. Scheeper, Wouter Olthuis, and Piet Bergveld

Abstract—**Silicon nitride corrugated diaphragms of 2 mm × 2 mm × 1 μm have been fabricated with 8 circular corrugations, having depths of 4, 10, or 14 μm. The diaphragms with 4-μm-deep corrugations show a measured mechanical sensitivity (increase in the deflection over the increase in the applied pressure) which is 25 times larger than the mechanical sensitivity of flat diaphragms of equal size and thickness. Since this gain in sensitivity is due to reduction of the initial stress, the sensitivity can only increase in the case of diaphragms with initial stress.**

A simple analytical model has been proposed that takes the influence of initial tensile stress into account. The model predicts that the presence of corrugations increases the sensitivity of the diaphragms, because the initial diaphragm stress is reduced. The model also predicts that for corrugations with a larger depth the sensitivity decreases, because the bending stiffness of the corrugations then becomes dominant. These predictions have been confirmed by experiments.

The application of corrugated diaphragms offers the possibility to control the sensitivity of thin diaphragms by geometrical parameters, thus eliminating the effect of variations in the initial stress, due to variations in the diaphragm deposition process and/or the influence of temperature changes and packaging stress.

I. Introduction

SILICON (condenser) microphones are provided with a thin diaphragm. Several diaphragm materials have been applied, as for example Mylar [1], [2], silicon nitride [3], [4], and silicon [5], [6]. The size of the diaphragms is typically between $1 \times 1\,\mathrm{mm}^2$ and $2 \times 2\,\mathrm{mm}^2$, with a typical thickness between 150 nm and 1 μm. The sensitivity of these thin diaphragms to a sound pressure (typically between 20 μPa and 20 Pa) is strongly dependent on the stress in the diaphragm. The tensile stress in thin silicon nitride films is typically of the order of 10^8 N/m^2 [7]. The stress in silicon diaphragms is determined by the diaphragm fabrication process. The tensile stress in heavily boron-doped silicon diaphragms is equal to 7×10^7 N/m^2 [6]. Bergqvist *et al.* [5] fabricated silicon diaphragms with a low doping level and a negligible stress.

In general, thin film microphone diaphragms show an initial stress which strongly determines the sensitivity of the microphone. The initial stress can be controlled within certain limits by the parameters of the deposition process. The run-to-run reproducibility is determined by the reproducibility of the initial conditions of the reactor (affected by contamination, adsorbed water, previously deposited layers) and the accuracy of the instruments which control the reactor temperature, the pressure and the mass flow of the process gases. Variations of a factor 2 of the initial stress have been measured.

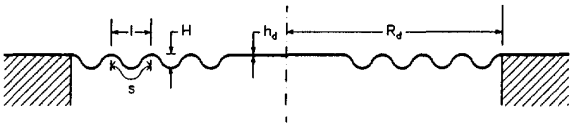

Fig. 1. Schematic cross-sectional view of a circular corrugated diaphragm and characteristic parameters.

It is advantageous if the mechanical sensitivity of the microphone diaphragms is not determined by deposition process parameters. A possible method to achieve this may be the application of a corrugated diaphragm, as shown in Fig. 1. In this figure, the corrugated diaphragm is provided with a flat center zone. It has first been shown by Jerman [8] that corrugated diaphragms can be made accurately in silicon using micromachining techniques. It has been calculated that a corrugated zone in a diaphragm can reduce stress with a factor 1000–10000 [9]. Therefore, one of the applications of corrugated diaphragms is the decoupling of a mechnical sensor from its encapsulation [9], [10], in order to reduce the influence of temperature changes and packaging stress. Recently, Spiering *et al.* [11] have demonstrated a reduction of thermal stress with at least a factor 120 in a corrugated diaphragm.

Flat diaphragms show a nonlinear relation between the deflection and the applied pressure. For relatively small deflections, this relation is approximately linear. The nonlinearity for large deflections is caused by stress due to stretching of the diaphragm. It has been experimentally shown that corrugated diaphragms have a larger linear range than flat diaphragms [8], [12], because of the achieved reduction of the radial stress in the diaphragm. The reduced influence of thermal stress and packaging stress, and the larger linear range compared with flat diaphragms, make the corrugated diaphragms attractive for specific applications, as for instance pressure sensors [8] and Fabry-Perot interferometers [13], [14].

The application of corrugated diaphragms in microphones or capacitive pressure sensors may offer the possibility to control the mechanical sensitivity of the diaphragm by means of the dimensions of the corrugations, which are often easier to control than the parameters of a deposition process. In

Manuscript received May 14, 1993; revised November 4, 1993. Subject Editor, N. de Rooij. This work was supported by the Dutch Foundation for Fundamental Research on Matter (FOM).

P. R. Scheeper was with the MESA Research Institute, University of Twente, 7500 AE Enschede, The Netherlands. He is now with Brüel and Kjaer, 2850 Naerum, Denmark.

W. Olthuis and P. Bergveld are with the MESA Research Institute, University of Twente, 7500 AE Enschede, The Netherlands.

IEEE Log Number 9215320.

this paper, the application of corrugated diaphragms for use in microphones is studied. Haringx [15] and Di Giovanni [16] have presented analytical models in which the effect of initial stress in the diaphragm is not included. The results of a finite element models describing the reduction of (thermal) stress by a corrugated zone were presented by Spiering *et al.* [9], by Ding [17], and by Zhang and Wise [8]. The deflection due to a homogeneous pressure was calculated by Ding [17] and by Zhang and Wise [18]. Unfortunately, the finite element calculations are only valid for a specific diaphragm geometry and size, and therefore the results cannot be applied to other diaphragms. In a recent paper, Spiering *et al.* [11] show that the flat center zone of a square diaphragm with a deep circular corrugation (deeper than 25 μm) can be modeled as a stress-free circular membrane with a clamped edge and free radial movement. In this paper, it will be shown that for a diaphragm with shallow corrugations, the initial stress has a considerable effect on the mechanical behavior of the diaphragm. An analytical model will be presented in Section II for circular corrugated diaphragms with initial stress. In Section III, the fabrication of corrugated diaphragms is discussed and in Section IV results of measurements are shown.

II. The Mechanical Sensitivity of Corrugated Diaphragms

The center deflection, w_0, of a flat, circular diaphragm with clamped edges and without initial stress, due to a homogeneous pressure, P, can be calculated from [8]

$$P = 5.33\frac{E_d}{(1-\nu^2)}\frac{h_d^4}{R_d^4}\frac{w_0}{h_d} + 2.83\frac{E_d}{(1-\nu^2)}\frac{h_d^4}{R_d^4}\frac{w_0^3}{h_d^3} \quad (1)$$

where E_d, ν, R_d, and h_d are the Young's modulus, the Poisson's ratio, the radius and the thickness of the diaphragm, respectively. It can be seen from (1) that if $(w_0/h_d) \ll 1$ the relation between the center deflection and the applied pressure is approximately linear. For larger values of (w_0/h_d) the relation is nonlinear. In (1) it is assumed that the initial diaphragm stress can be neglected.

Haringx [15] presented a model to calculate the deflection of circular, stress-free corrugated diaphragms. Di Giovanni [16] presented another set of equations, which are equal to the equations presented by Haringx for small diaphragm deflections, but provide a more accurate solution for large deflections (see the discussion on Fig. 11 in Section IV):

$$P = a_p E_d \frac{h_d^4}{R_d^4}\frac{w_0}{h_d} + b_p\frac{E_d}{(1-\nu^2)}\frac{h_d^4}{R_d^4}\frac{w_0^3}{h_d^3} \quad (2)$$

where

$$a_p = \frac{2(q+1)(q+3)}{3\left(1-\frac{\nu^2}{q^2}\right)} \quad (3)$$

$$b_p = 32\frac{1-\nu^2}{q^2-9}\left[\frac{1}{6} - \frac{3-\nu}{(q-\nu)(q+3)}\right] \quad (4)$$

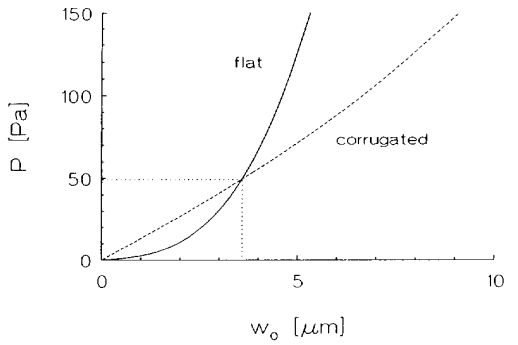

Fig. 2. Example of a pressure-deflection curve of a stress-free circular flat and corrugated diaphragm without a flat zone. For the value of the parameters, see text.

and for a sinusoidal corrugation profile

$$q^2 = \frac{S}{l}\left[1 + 1.5\frac{H^2}{h_d^2}\right] \quad (5)$$

where H is the depth of the corrugations, l is the corrugation spatial period, s is the corrugation arc length (see Fig. 1), and q is the corrugation profile factor, which is larger than 1 for corrugated diaphragms. For flat diaphragms $(H = 0), q$ is equal to 1.

In Section III it will be shown that the corrugated diaphragms that have been fabricated show a rectangular corrugation profile. However, for shallow corrugations $(H \ll 1)$, the shape of the corrugations has only little influence on the profile factor q [15], [16]. In (2)–(5), it is assumed that the corrugated diaphragm is not provided with a flat center zone, in contrast to the corrugated diaphragm which will be presented in Section III (see also Fig. 1). This can be compensated for in the factor s/l, representing the ratio of the real distance between the diaphragm center and the edge, measured along the corrugation profile, and the diaphragm radius:

$$\frac{S}{l} = \frac{R_d + 2NH}{R_d} \quad (6)$$

where N is the number of corrugations. Note that (6) is only valid for a rectangular corrugation profile.

In Fig. 2, typical load-deflections curves are shown for a *stress-free* flat and a stress-free (shallow) corrugated diaphragm without flat zone, according to (1) and (2). In this example, a Poisson's ratio of 0.3, a Young's modulus of 3×10^{11} N/m^2, a radius of 1 mm, a diaphragm thickness of 1 μm, and a corrugation depth of 5 μm have been assumed. The assumed Young's modulus is based on the processes used in our labs, yielding values of 3–4 $\times 10^{11}$ N/m^2.

If only *small* deflections are considered (smaller than 3.6 μm in Fig. 2), it can be seen that the corrugated diaphragm is stiffer than a flat diaphragm. This has been confirmed by experiments, as can, for instance, be found in [15]. The larger stiffness of the corrugated diaphragm is caused by the larger *flexural* rigidity in the tangential direction. The flexural rigidities in the radial direction, which depend on the thickness of the diaphragm material, are equal for the flat and the corrugated diaphragm. Note that bending occurs in the radial as well as the tangential

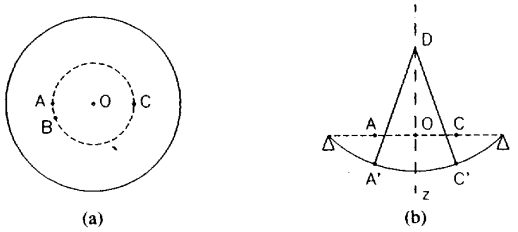

Fig. 3. A top view (a) and a cross-sectional view (b) of a deflected circular diaphragm.

direction. This can be elucidated with Fig. 3(a). Fig. 3(a) shows a top view of a circular stress-free diaphragm. The points A, B, and C are at equal distances from the diaphragm center O. Fig. 3(b) shows a diametrical cross-sectional view of the diaphragm. The z axis is an axis of rotational symmetry. It can be seen from Fig. 3(b) that the diaphragm shows a curvature in the radial direction. For small deflections of the stress-free diaphragm, the points A and C are displaced vertically and indicated as A' and C'. In the undeflected state, the normals from the points A, B, and C are all parallel to each other and perpendicular to the plane of the diaphragm. In the deflected state, the normals from the points A' and C' intersect the z axis at point D. Because of the rotational symmetry, the normals from all points at the same distance from the diaphragm center O form a conical surface with apex D. Therefore, considering the normals of the points A' and B', it can be concluded that the diaphragm also bends in the tangential direction.

In the case of *large* diaphragm deflections (larger than 3.6 μm in Fig. 2), the tensile stress that occurs due to stretching of a diaphragm can no longer be neglected. The resulting increase in the stiffness of a diaphragm causes the nonlinear behavior. Since the corrugated diaphragm shows a smaller *tensile* rigidity in the radial direction than a flat diaphragm, the stress and the nonlinearity in a corrugated diaphragm are smaller than in a flat diaphragm. The corrugated diaphragm has a smaller stiffness and shows a larger deflection than a flat diaphragm, considering the high-pressure range (higher than 50 Pa in Fig. 2). The large-deflection behavior has been demonstrated by Jerman for doped silicon corrugated diaphragms [8] and by Van Mullem for polyimide corrugated diaphragms [12].

The deflection of a corrugated diaphragm with initial stress can be approximated by means of an analytical expression, which is a superposition of the linear model of a corrugated diaphragm without initial stress, and the linear (flat) membrane model which assumes a high initial tensile stress. The superposition is based on the assumption that the corrugated diaphragm can be modelled as a fictitious flat diaphragm, which locally has the same radial and tangential flexural rigidity as the corrugated diaphragm [15]. An initial stress is assumed to act on the fictitious flat diaphragm. The initial stress is reduced by the presence of corrugations in the diaphragm. However, an estimate must be made of the reduction of the initial stress caused by the corrugations. Since the nonlinear behavior of diaphragm is caused by stress, and this nonlinearity is reduced by the presence of corrugations, the estimate can be made by considering the cubic terms in the pressure-deflection curves.

The stress, due to stretching of the middle plane of a diaphragm, can be estimated by considering the pressure-deflection curve of a diaphragm with a large initial stress [8]:

$$P = 4\frac{h_d^2}{R_d^2}\frac{w_0}{h_d}\left[\sigma_d + \frac{2.83}{4}\frac{E_d}{(1-\nu^2)}\frac{h_d^2}{R_d^2}\frac{w_0^2}{h_d^2}\right] \tag{7}$$

where σ_d is the initial stress in the diaphragm. This equation has been rewritten so that it can be seen that the second term between the brackets represents the stress that is caused by stretching of the middle plane of the diaphragm. Equation (1), the pressure-deflection curve for a flat diaphragm without initial stress, can be rewritten in a similar way as (7). The second term between the brackets is then exactly the same as in (7) and also represents the stress that is caused by stretching of the middle plane of the diaphragm.

Rewriting (2), the pressure-deflection curve for a corrugated diaphragm without initial stress, gives

$$P = 4\frac{h_d^2}{R_d^2}\frac{w_0}{h_d}\left[\frac{a_p}{4}E_d\frac{h_d^2}{R_d^2} + \frac{b_p}{4}\frac{E_d}{(1-\nu^2)}\frac{h_d^2}{R_d^2}\frac{w_0^2}{h_d^2}\right] \tag{8}$$

Comparing the second term between the brackets of (8) and (7), it can be seen that the stress, due to stretching of the middle plane, has been reduced with a factor $b_p/2.83$ in the corrugated diaphragm. Thus, if the behavior of a corrugated diaphragm with initial stress is described using superposition of a stress-free corrugated diaphragm and a flat diaphragm with initial stress, a flat diaphragm with an initial stress of $\sigma_d b_p/2.83$ instead of σ_d should be considered. Since superposition is only valid for linear systems, only the linear terms of (7) and (8) are used. Thus, the following equation is obtained:

$$P = 4\frac{h_d^2}{R_d^2}\frac{w_0}{h_d}\left[\sigma_d\frac{b_p}{2.83} + \frac{a_p}{4}E_d\frac{h_d^2}{R_d^2}\right]. \tag{9}$$

The mechanical sensitivity of a circular diaphragm is defined as

$$S_m = \frac{dw_0}{dP} \tag{10}$$

Therefore, the mechanical sensitivity of the corrugated diaphragm with initial stress, for small deflections, is given by

$$S_m = \frac{R_d^2}{4h_d\left[\sigma_d\frac{b_p}{2.83} + \frac{a_p}{4}E_d\frac{h_d^2}{R_d^2}\right]}. \tag{11}$$

The behavior of a corrugated diaphragm is determined by the profile factor q. The number of corrugations, N, has only little influence on the profile factor (see (5) and (6)), whereas q is nearly proportional with the corrugation depth, H (see (5)). Therefore, the corrugation depth is the most effective parameter to influence the behavior of corrugated diaphragms.

In Fig. 4 the mechanical sensitivity for small deflections of corrugated diaphragms without a flat zone is shown as a function of the corrugation depth, H, for diaphragms with an initial stress of $10^7\ \mathrm{N/m^2}(b)$ and $10^8\ \mathrm{N/m^2}(c)$ (equation (11)),

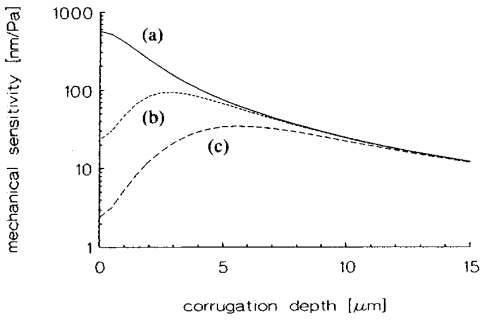

Fig. 4. The mechanical sensitivity of a corrugated diaphragm (without a flat zone) without initial stress (a) and with an initial stress of 10^7 N/m^2 (b) and 10^8 N/m^2 (c).

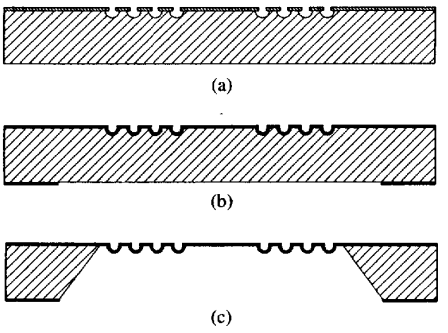

Fig. 5. Schematic representation of the fabrication process of corrugated diaphragms with a flat zone.

and for the stress-free case (a) (equation (2)). A Poisson's ratio of 0.3, a Young's modulus of 3×10^{11}N/m^2, a radius of 1 mm, and a diaphragm thickness of 1 μm have been assumed. Note that for flat diaphragms ($H = 0$) the mechanical sensitivity reduces drastically if the initial stress increases.

For stress-free corrugated diaphragms the mechanical sensitivity decreases if the corrugation depth increases. For the corrugated diaphragms with initial stress the mechanical sensitivity increases for small corrugation depths, due to reduction of the initial stress. For relatively large corrugation depths, the mechanical sensitivity decreases for increasing corrugation depths and approaches asymptotically the curve for stress-free corrugated diaphragms. The mechanical sensitivity of the diaphragm is then determined by geometrical parameters and not by the initial stress. It can be seen in the example from Fig. 4 that this is achieved for a corrugation depth larger than 10 μm. The ratio of the mechanical sensitivities of the diaphragms with an initial stress of 10^7 N/m^2 (b) and 10^8 N/m^2 (c) has been reduced from a factor 10, for flat diaphragms, to a factor 1.10, for diaphragms with a corrugation depth of 10 μm. Therefore, in this example it may be expected that variations in the initial stress in the diaphragm material have a negligible effect on the resulting mechanical sensitivity of a corrugated diaphragm with a corrugation depth of at least 10 μm. Another advantage of the application of corrugated diaphragms is that if the initial stress is equal to 10^8 N/m^2 (c), the mechanical sensitivity is increased with a factor of about 10.

III. The Fabrication of Corrugated Diaphragms

The fabrication process of LPCVD silicon nitride corrugated diaphragms with a flat zone is schematically shown in Fig. 5(a)–(c):

(a) Corrugations with a depth of 4, 10, 14, and 19 μm have been etched in a 3-in p-type, < 100 >-oriented silicon wafer using a 0.5-μm-thick evaporated aluminum etch mask and reactive ion etching (RIE) in an SF_6-O_2 plasma.

(b) After removal of the aluminum etch mask, 1 μm of low pressure chemical vapor deposited (LPCVD) silicon nitride is deposited on both sides of the wafer. Square windows are etched in the silicon nitride on the reverse side of the wafer using RIE in a CHF_3/O_2 plasma.

Fig. 6. SEM photograph of a square silicon nitride diaphragm with a square corrugation pattern.

(c) Square diaphragms are made by anisotropic etching from the reverse side of the wafer in a 33 wt% KOH solution (73°C), using the LPCVD silicon nitride on the reverse side of the wafer serves as an etch mask.

This process was developed by Spiering *et al.* [19], who fabricated corrugated diaphragms with a square boss/diaphragm structure in the center.

Since the diaphragms are fabricated on < 100 > silicon, only square diaphragms can be etched. However, the corrugations can be etched in square or circular patterns. Fig. 6 shows an example of a corrugated diaphragm with corrugations in a square pattern. The corrugation depth is about 19 μm. It was found that this type of diaphragm was very vulnerable and the diaphragms were damaged very easily. This is probably caused by high local stresses at the sharp corners of the corrugations.

Fig. 7 shows a 2×2 mm^2 square diaphragm with corrugations in a circular pattern. A cross-sectional view of a detail of the diaphragm is shown in Fig. 8. It was found that this type of diaphragm was robust and could withstand the handling and dicing of the wafer. Therefore, this type of diaphragm was used for further testing. The diaphragms with different corrugation depths were fabricated on separate wafers. Each wafer was provided with flat diaphragms, which were used as a reference.

Note that all corrugated diaphragms are provided with 8 corrugations and a flat center zone. The flat zone is meant

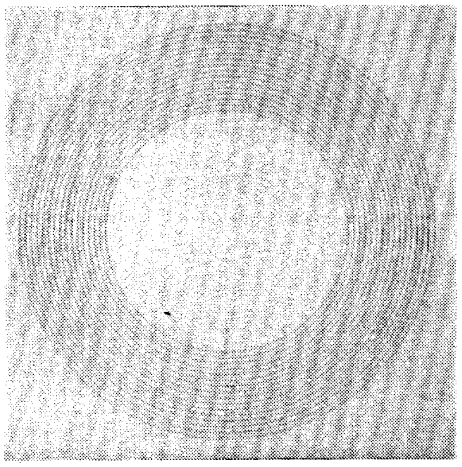

Fig. 7. Top view of a 2 mm × 2 mm × 1 μm silicon nitride diaphragm with a circular corrugation pattern. The diaphragm is backside illuminated.

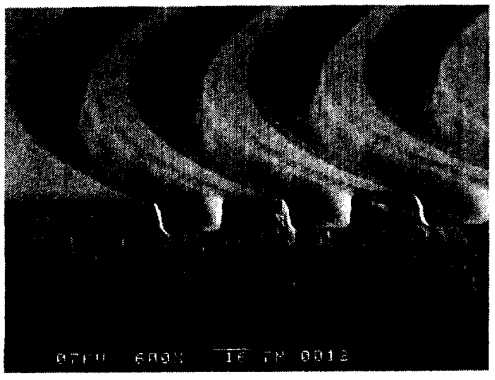

Fig. 8. SEM photograph of a detail of the cross-sectional view of a corrugated diaphragm, as shown in Fig. 7. The silicon substrate has not been etched for obvious reasons of mechanical integrity.

for reliable deflection measurements, because the deflection is measured by means of a mechanical scan with a surface profiler. The width of the corrugations is 25 μm and the separation between two corrugations is also 25 μm, giving a corrugation period of 50 μm, as can be seen from Fig. 8. The excellent step coverage of the LPCVD silicon nitride is also shown in Fig. 8.

IV. Measurement Results

The mechanical sensitivity of all diaphragms was measured using the bulge test, as for instance described by Bromley *et al.* [20]. For this purpose, the samples with a diaphragm were mounted on special holders. A homogeneous pressure was applied to the samples using a Wallace & Tiernan Chlorator FA-235-G pressure controller. The diaphragm deflection was measured using a DEK-TAK 3030 surface profiler. A stylus force of 1×10^{-5} N was used for the flat diaphragms, whereas the stylus force was 5×10^{-5} N for the corrugated diaphragms. In the latter case, a larger force was necessary to provide sufficient damping of the movement of the stylus when it scanned the corrugations.

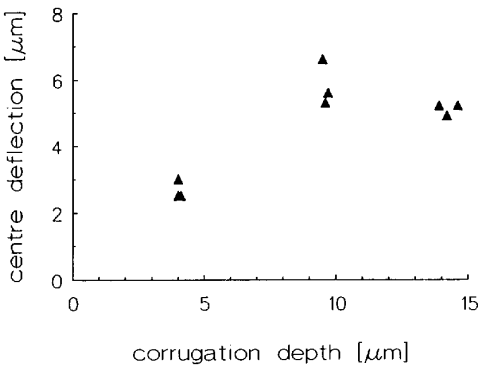

Fig. 9. The measured static center deflection of corrugated diaphragms as a function of the corrugation depth.

It was found that the corrugated diaphragms, which were not loaded by any external force, showed a spontaneous static deflection. The finite element calculations of Spiering *et al.* [9], Ding [17], and Zhang and Wise [18] have indicated that the presence of a tensile or compressive stress in the corrugated diaphragm causes this spontaneous deflection. Note that this spontaneous deflection is different from buckling, which is a spontaneous deformation due to a too high compressive stress. Buckling occurs only in case of compressive stress and only if the compressive stress has exceeded a critical value. The direction into which a buckled diaphragm deforms, and the shape of a buckled diaphragm cannot be exactly predicted. Spiering *et al.* [9], Ding [17], and Zhang and Wise [18] have shown that the direction and magnitude of the spontaneous deflection of a corrugated diaphragm can, in principle, be calculated if the dimensions and the stress are known.

If Fig. 9 the measured values of the spontaneous center deflection are given as a function of the corrugation depth. These values have been obtained by measuring the centre deflection of the diaphragm with stylus forces between 1×10^{-5} N and 5×10^{-5} N, and subsequently extrapolating the deflections to the value which is expected at a stylus force of 0 N, using a linear least squares fit. All diaphragms showed an upward static deflection. The spreading of the measured deflections is mainly due to the vibration of the diaphragm, which occurs if relatively low stylus forces are used for scanning the corrugated diaphragm. Larger stylus forces have not been used to avoid possible damage to the diaphragms.

Since all types of diaphragms show a similar pressure-deflection curve, as can be seen from the (1), (2), and (7), the measured values of the center deflection for different applied pressures were fitted to the curve

$$P = A(w_{0,m} - w_s)^3 + B(w_{0,m} - w_s) \qquad (12)$$

where A and B are curvefit coefficients and $w_{0,m}$ and w_s are the measured diaphragm center deflection and the static center deflection, respectively. Note that w_s is not the extrapolated spontaneous center deflection, as shown in Fig. 9, but is the result of the spontaneous center deflection, as well as the deflection due to the stylus force of 5×10^{-5} N. It can

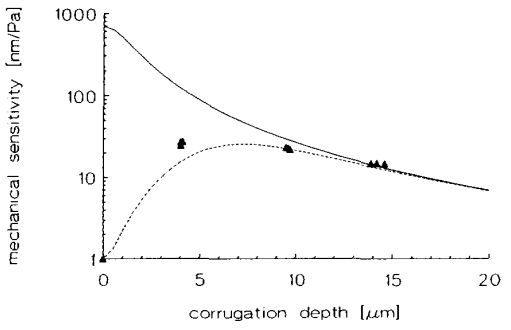

Fig. 10. The measured mechanical sensitivity of corrugated diaphragms as a function of the corrugation depth (markers) and theoretically expected values for an initial stress of 3.1×10^8 N/m^2 (– – –) and for the stress-free case (——).

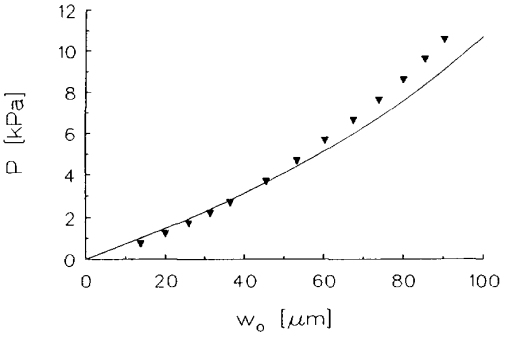

Fig. 11. The measured pressure-deflection curve for a diaphragm with 14-μm-deep corrugations (markers) and the theoretically expected values according to the model of Di Giovanni [16] (line).

be concluded from the (10) and (12) that the mechanical sensitivity for small diaphragm center deflections, where the relation between P and $(w_{0,m} - w_s)$ is approximately linear, is given by

$$S_m = \frac{dw_0}{dP} = \frac{1}{B}. \tag{13}$$

Equations (12) and (13) are used to calculate the mechanical sensitivity for small deflections from the measured pressure-deflection curves.

In Fig. 10 the measured mechanical sensitivities are shown as a function of the corrugation depth. An initial stress of 3.1×10^8 N/m^2 and a Young's modulus of 4.0×10^{11} N/m^2 have been obtained from the measurements on flat diaphragms. The theoretically expected sensitivities are shown for corrugated diaphragms with and without initial stress, based on the measured stress and Young's modulus. A Poisson's ratio of 0.3 is assumed. For the calculations an effective diaphragm radius $R = a/\sqrt{\pi}$ has been used. For a diaphragm with a side length a of 2 mm the effective diaphragm radius becomes 1.13 mm.

It can be concluded from Fig. 10 that the measured mechanical sensitivities are in a good agreement with the theoretically predicted values, although in the theory it was assumed that the diaphragms are circular and the stress reduction was only a rough estimate. A corrugation depth of 4 μm increases the mechanical sensitivity from 1.0 nm/Pa, for flat diaphragms, to about 25 nm/Pa. The mechanical sensitivities of the diaphragms with a corrugation depth of about 14 μm (15 nm/Pa) agree reasonably with the mechanical sensitivity predicted by the stress-free model.

In the case that the initial stress has been reduced considerably (nearly stress-free diaphragm), the mechanical sensitivity is inversely proportional to the value of the Young's modulus (see (11)). However, the Young's modulus is less dependent on process parameters than the initial stress [21].

Fig. 11 shows the measured pressure-deflection curve of a diaphragm with 14 μm-deep corrugations (markers) and the theoretically predicted values according to the model of Di Giovanni [16] ((2)-(5)), which is valid for stress-free corrugated diaphragms. Although in the low-pressure region the model agrees reasonably with the measured values, the pressures corresponding to large deflections are notably larger than predicted. For example, at a deflection of 90 μm the required pressure according to the model of Di Giovanni is 9.0 kPa, whereas 10.5 kPa was measured. The model of Haringx [15], which has been used by Jerman [8], predicts a pressure of 17 kPa.

V. Conclusions

Silicon nitride corrugated diaphragms of 2 mm × 2 mm × 1 μm have been fabricated. The diaphragms were provided with 8 circular corrugations with depths of 4, 10, or 14 μm. It was found that the behavior of the corrugated diaphragms was strongly influenced by the initial stress. The measured mechanical sensitivity was considerably lower than the values that were predicted by the model of Di Giovanni [16], which assumed a stress-free diaphragm. A model has been proposed that takes the influence of tensile stress into account. This model is a super-position of the model of a stress-free corrugated diaphragm and a diaphragm with a high initial tensile stress. The reduction of the initial stress was estimated from the change in the cubic terms in the load-deflection equations from the stress-free flat and corrugated diaphragm.

The model predicts that the mechanical sensitivity increases for small corrugation depths, due to the reduction of the initial diaphragm stress. For large corrugation depths, the mechanical sensitivity decreases, due to the stiffening effect of the corrugations. Both effects have been confirmed by experiments. For large corrugation depths, the mechanical sensitivity is only weakly depending on the initial stress and becomes equal to the value predicted by the stress-free model.

It can be concluded that analytical models have been presented for corrugated diaphragms for three different cases. First, the models of Haringx [15] and Di Giovanni [16] for stress-free (shallow) corrugated diaphragms. Next, the model of Spiering *et al.* [11] for a diaphragm with a (single) deep corrugation with initial tensile stress, which can be considered as if it is stress-free. Finally, our model describes the intermediate case of diaphragms with shallow corrugations and with initial stress.

All tested corrugated diaphragms showed a static center deflection without applying any load. This static center de-

flection of 2 to 7 μm should be taken into account when designing microphones with a corrugated diaphragm. A solution is to eliminate the static center deflection by fabricating corrugations that are symmetrical about the central plane of the diaphragm [18].

Summarizing, the mechanical sensitivity of diaphragms with initial tensile stress can be increased considerably by providing the diaphragm with corrugations. Furthermore, corrugated diaphragms offer the possibility to make the mechanical sensitivity of diaphragms independent of variations in the initial stress, caused by variations of deposition process parameters.

ACKNOWLEDGMENT

The authors would like to thank P. Bakker for producing and testing the corrugated diaphragms with a square corrugation pattern, B. Otter for producing the SEM photographs, H. van Vossen for growing the LPCVD silicon nitride layers and H. Voorthuyzen, V. Spiering, and R. Spiering for useful suggestions and discussions.

REFERENCES

[1] D. Hohm and R. Gerhard-Multhaupt, "Silicon-dioxide electret transducer," *J. Acoust. Soc. Amer.*, vol. 75, pp. 1297–1298, 1984.

[2] A. J. Sprenkels, R. A. Groothengel, A. J. Verloop. and P. Bergveld, "Development of an electret microphone in silicon," *Sensors and Actuators*, vol. 17. pp. 509–512, 1989.

[3] D. Holm and G. Hess, "A subminiature condenser microphone with silicon nitride membrane and silicon backplate," *J. Acoust. Soc. Amer.*, vol. 85, pp. 476–480, 1989.

[4] W. Kühnel and G. Hess, "Micromachined subminiature condenser microphones in silicon," *Sensors and Actuators A*, vol. 32, pp. 560–564, 1992.

[5] J. Bergqvist, F. Rudolf, J. Maisano, F. Parodi, and M. Rossi, "A silicon condenser microphone with a highly perforated backplate," in *Dig. Tech. Papers, Transducers '91*, San Francisco, CA, June 1991, pp. 266–269.

[6] T. Bourouina, S. Spirkovitch, F. Baillieu, and C. Vauge, "A new microphone with a p^+ silicon membrance," *Sensors and Actuators A*, vol. 31, pp. 149–152, 1992.

[7] P. R. Scheeper, J. A. Voorthuyzen, and P. Bergveld, "PECVD silicon nitride diaphragms for condenser microphones," *Sensors and Actuators B*, vol. 4, pp. 79–84, 1991.

[8] J. H. Jerman, "The fabrication and use of micromachined corrugated silicon diaphragms," *Sensors and Actuators*, vol. A21–A23, pp. 988–992, 1990.

[9] V. L. Spiering, S. Bouwstra, R. M. E. J. Spiering, and M. Elwenspoek, "On-chip decoupling zone for package-stress reduction," in *Dig. Tech. Papers, Transducers '91*, San Francisco, CA, June 1991, pp. 982–985.

[10] H. L. Offereins, H. Sandmaier, B. Folkmer, U. Steger, and W. Lang, "Stress free assembly technique for a silicon based pressure sensor," in *Dig. Tech. Papers, Transducers '91*, San Francisco, CA, June 1991, pp. 986–989.

[11] V. L. Spiering, S. Bouwstra, J. Burger, and M. Elwenspoek, "Membranes fabricated with a deep single corrugation for package stress reduction and residual stress relief," in *Dig. Tech. Papers, MicroMechanics Europe Workshop (MME'93)*, Neuch\^atel, Switzerland, Sept. 1993, pp. 223–227.

[12] C. J. van Mullem, K. J. Gabriel, and H. Fujita, "Large deflection performance of surface micromachined corrugated diaphragms," in *Dig. Tech. Papers, Transducers '91*, San Francisco, CA, June 1991, pp. 1014–1017.

[13] J. H. Jerman, D. J. Clift, and S. R. Malinson, "A miniature Fabry-Perot interferometer with a corrugated silicon diaphragm support," in *Dig. Tech. Papers, IEEE Solid-State Sensor and Actuator Workshop*, Hilton Head Island, SC, June 1990, pp. 140–144.

[14] N. F. Raley, D. R. Ciarlo, J. C. Koo, B. Beiriger, J. Trujillo, C. Yu, G. Loomis, and C. R. Chow, "A Fabry-Perot microinterferometer for visible wavelengths," in *Dig. Tech. Papers, IEEE Solid-State Sensor and Actuator Workshop*, Hilton Head Island, SC, June 1992, pp. 170–173.

[15] J. A. Haringx, "Design of corrugated diaphragms," *ASME Trans.*, vol. 79, pp. 55–64, 1957.

[16] M. Di Giovanni, *Flat and Corrugated Diaphragm Design Handbook*, 1st ed. New York: Marcel Dekker, 1982, pp. 255–262.

[17] X. Ding, "Behavior and application of silicon diaphragms with a boss and corrugations," in *Dig. Tech. Papers, IEEE Solid-State Sensor and Actuator Workshop*, Hilton Head Island, SC, June 1992, pp. 166–169.

[18] Y. Zhang and K. D. Wise, "Performance of nonplanar silicon diaphragms under large deflections," in *Dig. Tech. Papers, IEEE Micro Electromechanical Systems Workshop*, Fort Lauderdale, FL, Feb. 1993, pp. 284–288.

[19] V. L. Spiering, S. Bouwstra and J. H. J. Fluitman, "Realization of mechanical decoupling zones for package-stress reduction," *Sensors and Actuators A*, vol. 37–38, pp. 800–804, 1993.

[20] E. L. Bromley, J. N. Randall, D. C. Flanders, and R. W. Mountain, "A technique for the determination of stress in thin films," *J. Vac. Sci. Technol. B*, vol. 1, pp. 1364–1366, 1983.

[21] S. Bouwstra, "A resonating microbridge mass flow sensor," Ph.D. dissertation, Univ. of Twente, 1990, pp. 52-55.

Patrick R. Scheeper was born in Nieuw Vennep, The Netherlands, on October 25, 1965. He received the B.S. degree in applied physics from the Rooms Katholieke Hogere Technische School Rijswijk, Rijswijk, The Netherlands, in 1988 and the Ph.D. degree from the Bio-Information Group, Department of Electrical Engineering, University of Twente, The Netherlands, in 1993. His current research is focused on the development of a microphone based on silicon technology for use in hearing aids.

Wouter Olthuis was born in Apeldoorn, The Netherlands, on October 23, 1960. He received the M.S. degree in electrical engineering from the University of Twente, Enschede, The Netherlands, in 1986, and the Ph.D. degree from the Biomedical Engineering Division of the Faculty of Electrical Engineering, University of Twente, Enschede, The Netherlands, in 1990.

Currently, he is working as an Assistant Professor in the Biosensor Technology Group of the University of Twente.

Piet Bergveld was born in Oosterwolde, The Netherlands, on January 26, 1940. He received the M.S. degree in electrical engineering from the University of Eindhoven, The Netherlands, in 1965 and the Ph.D. degree from the University of Twente, The Netherlands, in 1973.

Since 1965 he has been a member of the Biomedical Engineering Division of the faculty of Electrical Engineering, University of Twente, and was in 1984 appointed as Professor in Biosensor Technology. He is one of the project leaders in the MESA Research Institute. His research subjects concern the further development of ISFET's and biosensors based on ISFET technology as well as silicon microphones. He has written more than 150 papers on these topics.